DEEP LEARNING-BASED QUASI-CONFORMAL SURFACE REGISTRATION FOR PARTIAL 3D FACES APPLIED TO FACIAL RECOGNITION

A PREPRINT

Yuchen Guo
Department of Mathematics
The Chinese University of Hong Kong

Hanqun Cao
Department of Mathematics
The Chinese University of Hong Kong

Lok Ming Lui
Department of Mathematics
The Chinese University of Hong Kong

ABSTRACT

3D face registration is an important process in which a 3D face model is aligned and mapped to a template face. It has significant applications in various fields, including facial recognition, animation, virtual reality, and medical imaging. However, the task of 3D face registration becomes particularly challenging when dealing with partial face data, where only limited facial information is available. To address this challenge, this paper presents a novel deep learning-based approach that combines quasi-conformal geometry with deep neural networks for partial face registration. The proposed framework begins with a Landmark Detection Network (LD-Net) that utilizes curvature information to detect the presence of facial features and estimate their corresponding coordinates. These facial landmark features serve as essential guidance for the subsequent registration process. To establish a dense correspondence between the partial face and the template surface, a registration network based on quasiconformal theories is employed. The registration network establishes a bijective quasiconformal surface mapping aligning corresponding partial faces based on detected landmarks and curvature values. It consists of the Coefficients Prediction Network (CP-Net), which outputs the optimal Beltrami coefficient representing the surface mapping. The Beltrami coefficient quantifies the local geometric distortion of the mapping. By controlling the magnitude of the Beltrami coefficient through a suitable activation function, the bijectivity and geometric distortion of the mapping can be effectively controlled. The optimal Beltrami coefficient is then fed into the Beltrami solver network to reconstruct the corresponding mapping. The surface registration enables the acquisition of corresponding regions and the establishment of point-wise correspondence between different partial faces, facilitating precise shape comparison through the evaluation of point-wise geometric differences at these corresponding regions. Experimental results demonstrate the effectiveness of the proposed method in achieving accurate landmark detection and surface registration on partial faces, as well as performing shape comparison amongst them with a high accuracy.

Keywords Facial landmark detection · surface registration · quasi-conformal geometry · convolutional neural networks

1 Introduction

The shape analysis of the human face has garnered significant interest among researchers, emerging as a captivating and widely explored field of study[29, 4, 9]. It holds significant importance across diverse domains such as computer vision, computer graphics, and medical imaging, where it finds extensive applications. In computer vision, facial shape analysis plays a pivotal role in tasks such as facial recognition and facial expression analysis[41, 31, 22, 45, 36]. Similarly, in the realm of medical imaging, the analysis of facial shape proves invaluable in medical diagnosis and treatment planning[7].

2D facial analysis has been extensively studied and is the subject of a surplus of literature. Nevertheless, recent advancements in 3D acquisition devices have revolutionized the field by facilitating the availability of rich 3D data of human faces. This surpasses the limitations of 2D images by providing a wealth of geometric information. Notably, numerous mathematical models for 3D facial analysis have been developed, yielding promising results[20, 24, 32]. A critical step in conducting shape analysis of 3D faces involves establishing accurate and dense pointwise correspondence among different human faces. This dense correspondence permits systematic and quantitative comparison, enabling comprehensive shape analysis[35, 48]. While 3D surface registration of complete faces has been extensively studied, real-world scenarios often present challenges such as occlusions, partial view angles, or self-occlusions caused by hands or accessories. When faced with limited data availability, achieving correspondence between 3D partial faces becomes a more intricate task, commonly referred to as the *partial face registration* problem. The challenge lies in accurately determining the corresponding regions between two partially observed faces and establishing point-wise correspondence between these regions[50, 8, 18]. This particular class of surface registration problem is comparatively less studied. Without precise registration between partial faces, shape analysis and comparison among them cannot be performed accurately.

In this paper, we introduce a novel deep learning-based method that addresses the challenge of partial face registration. Our approach combines quasiconformal theories and deep neural networks to achieve accurate landmark detection and surface registration, even when dealing with partial facial data. This method can be further applied to facial recognition tasks. Our framework begins with a Landmark Detection Network (LD-Net), which precisely detects landmarks on the partial face surfaces using the curvature values derived from each vertex. This innovative approach allows us to accurately locate facial landmarks, even in scenarios with limited facial information or occlusions. These detected facial landmarks play a crucial role in guiding the subsequent registration process. To establish a dense correspondence between the partial face and the template surface, we employ a registration network based on quasiconformal theories. This network consists of the Coefficients Prediction Network (CP-Net), which outputs the optimal Beltrami coefficient representing the surface mapping. The Beltrami coefficient quantifies the local geometric distortion of the mapping. By controlling the magnitude of the Beltrami coefficient through a suitable activation function, we can effectively control the bijectivity and geometric distortion of the mapping. The optimal Beltrami coefficient is then fed into the Beltrami solver network to reconstruct the corresponding mapping. The surface registration achieved by our method enables the acquisition of corresponding regions and the establishment of point-wise correspondence between different partial faces. This facilitates precise shape comparison by evaluating point-wise geometric differences at these corresponding regions. To thoroughly evaluate the effectiveness of our proposed method, we conducted extensive experiments on partial facial surfaces. The results obtained from these experiments provide strong evidence for the robustness and reliability of our approach in achieving accurate landmark detection and surface registration for partial faces. The results of facial classification using the partial face registration further demonstrate the effectiveness of our proposed framework for analyzing partial faces.

In summary, the contribution of our work is as follows:

(I) Automatic extraction of feature landmarks on partial faces: We propose a deep neural network that automatically extracts feature landmarks on partial faces by leveraging surface curvature information. The network accurately identifies their presences and precise locations, thereby facilitating subsequent registration.

(II) Quasi-conformal deep neural network for 3D partial face registration: We propose a novel approach that combines quasi-conformal (QC) geometry with convolutional neural networks (CNNs) to address the challenge of registering partial face surfaces. By integrating these techniques, we can improve both the accuracy and efficiency of the registration process, even in the presence of occlusions or limited facial information.

(III) Facial recognition of partial faces: By achieving precise surface registration of partial faces, we can identify the overlapping regions on each partial face and establish point-wise correspondences between them. This facilitates shape comparison and enables the recognition of partial faces through the evaluation of geometric differences at key feature landmarks.

2 Related Works

2.1 Quasi-Conformal Mapping

Surface parameterization and mapping problems are widely investigated, and algorithms have been proposed in recent decades [15, 38]. In particular, as conformal maps preserve the local geometry, researchers developed algorithms that could be applied to various fields [11, 26, 33, 47]. However, the computation of conformal mapping is expensive and quasi-conformal theory has been found useful with trade-offs between conformality and other prescribed constraints [19,

25]. The Beltrami coefficient is introduced to measure the distortion of the mapping. In [16], Gardiner et al. proved the 1-1 correspondence between Beltrami coefficients and surface diffeomorphisms.

The utilization of quasi-conformal geometry in registration tasks allows for the alignment of different surfaces by minimizing distortion, which enables accurate and consistent alignment, even when dealing with complex deformations and variations in shape. In segmentation, quasi-conformal geometry has been applied to delineate boundaries and segment regions of interest by leveraging the topological properties of the underlying complex domains. Additionally, shape-matching techniques based on quasi-conformal geometry enable efficient and effective matching of shapes by preserving their local geometric properties.

By incorporating quasi-conformal geometry into our approach, we leverage its robustness and versatility to achieve accurate and reliable registration of partial face surfaces. This enables us to align and integrate partial faces with minimal distortion, facilitating subsequent analysis and recognition tasks.

2.2 Facial Landmark Detection

Facial landmark detection plays a crucial role in facial analysis as it provides key points representing anatomical structures, facial features, and regions of interest for various high-level tasks such as face recognition, registration, and editing [45]. Traditional methods for landmark detection rely on machine learning algorithms, including Support Vector Machines (SVM) [43] and Random Forests (RF) [28], using manually crafted key points. However, these approaches require expert annotations and have limited generalization capabilities across different datasets.

Recent advancements in landmark detection leverage the powerful feature extraction capabilities of Convolutional Neural Networks (CNN) to perform unsupervised landmark detection [23, 5]. To further improve detection accuracy and generalization abilities, researchers have proposed improved network architectures [53, 51], learning patterns [49], and well-designed loss functions [14, 44]. However, these existing approaches still face challenges in identifying facial landmarks with significant variations or on partial faces.

In this work, we present our landmark detection network specifically designed for partial human faces with diverse variations. Our network addresses the limitations of existing methods by effectively detecting landmarks on partial faces, thereby providing crucial information for subsequent registration processes.

2.3 Facial Registration

Traditional face registration methods primarily focus on aligning distorted facial landmarks with their corresponding landmarks using CNN-based networks and L2 loss [50]. These methods often incorporate advanced techniques such as inception blocks [39] and siamese networks [37, 40] to extract multi-scale features and learn discriminative embeddings. To handle variations in facial landmarks, techniques like wing loss and triplet loss have been proposed. 3D surface registration methods have also been developed to address non-linear distortions. These methods[46, 42] utilize 3D models to capture complex facial deformations.

However, acquiring a complete face for registration purposes can be challenging, leading to a growing interest in methods for partial surface registration. In recent years, several approaches have been proposed to tackle this problem. In [6], Cao et al. introduced a method that utilizes deep functional maps for unsupervised training to achieve shape correspondence even for partial shapes. Bracha et al. proposed a novel idea in [3], where they establish a direct correspondence between partial and full face shapes through feature matching. These recent advancements in the field of partial face registration highlight the growing interest in finding effective solutions for this challenging problem. However, existing research often lacks focus on the analysis of face surfaces. Consequently, the challenges associated with feature extraction and region correspondence for partial faces remain a significant problem that requires further attention and investigation.

To address this challenge, we propose a quasi-conformal-based registration model for partial faces' correspondence. Our model combines the benefits of quasi-conformal methods while handling partial components and non-rigid deformations, filling the existing gaps in face registration research.

3 Mathematical Background

3.1 Quasi-conformal theory

In this section, we introduce the theories related to quasi-conformal maps. For more details, please refer to [2, 16].

Compared with the conformal map, the quasi-conformal map is more generalized and can be understood to be a map with bounded conformality distortion. An orientation-preserving homeomorphism $f : \Omega \subset \mathbb{C} \to \Omega' \subset \mathbb{C}$ is said to be a quasi-conformal map if it satisfies the Beltrami equation:

$$\frac{\partial f}{\partial \bar{z}} = \mu_f(z)\frac{\partial f}{\partial z}, \tag{1}$$

where $\mu_f(z)$ is a complex-valued Lebesgue-measurable function satisfying $\|\mu_f(z)\|_\infty < 1$ is the Beltrami coefficient of f and it represents the conformality distortion of f.

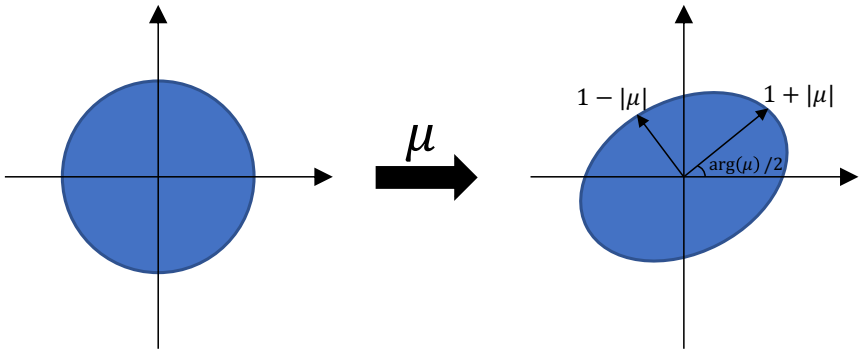

Figure 1: The illustration of how Beltrami coefficient μ determine the conformal distortion.

If we are given a Beltrami coefficient μ with $\|\mu\|_\infty < 1$, we can solve its corresponding quasi-conformal mapping satisfying the Beltrami equation[16].

Theorem 1. *Suppose $\mu : \mathbb{D} \to \mathbb{C}$ is Lebesgue measurable with $\|\mu\|_\infty < 1$. There is a quasi-conformal homeomorphism ϕ from $\mathbb{D}$ to itself, which is in the Sobolev space $W^{1,2}(\mathbb{D})$ and satisfies the Beltrami equation (1) in the distribution sense. Furthermore, by fixing 0 and 1, ϕ is uniquely determined.*

Conversely, if an orientation preserving homeomorphism ϕ is preseted, we can get its Beltrami coefficient by:

$$\mu_\phi = \frac{\partial \phi}{\partial \bar{z}} \Big/ \frac{\partial \phi}{\partial z}. \tag{2}$$

Thus, the Jacobian Matrix J of ϕ can be expressed according to μ_ϕ as follows:

$$J(\phi) = \left|\frac{\partial \phi}{\partial z}\right|^2 \left(1 - |\mu_\phi|^2\right). \tag{3}$$

Given that ϕ is an orientation preserving homeomorphism, $J(\phi) > 0$ and $|\mu_\phi| < 1$ everywhere. Hence, $\|\mu_\phi\|_\infty < 1$ should hold. Theorem 1 indicates that under suitable normalization, every μ with $\|\mu\|_\infty < 1$ is associated with a unique homeomorphism. Therefore, a homeomorphism from $\mathbb{C}$ or $\mathbb{D}$ onto itself can be uniquely determined by its associated Beltrami coefficient.

In addition, we can also composite two quasi-conformal maps and the Beltrami coefficient can be computed. Suppose we have f, g: $\mathbb{C} \to \mathbb{C}$, two quasi-conformal maps, associated with Beltrami coefficients μ_f and μ_g respectively. Thus, the Beltrami coefficient of $g \circ f$ is

$$\mu_{g\circ f} = \frac{\mu_f + (\mu_g \circ f)\tau}{1 + \bar{\mu}_f(\mu_g \circ f)\tau}, \tau = \frac{\bar{f}_z}{f_z} \tag{4}$$

3.2 Conformal Parameterization

In this section, we are going to introduce the variational formulation of the conformal parameterization from [11].

Suppose we have a piecewise linear mesh patch M and we want to construct a piecewise linear mapping ψ between M and a planar triangulation $U \in \mathscr{R}$ conformally. We denote x_i to be 3D positions of the i-th vertex on M and u_i is its corresponding position on U.

In [11], they introduced the Dirichlet energy and Chi energy on triangulations.

$$E_A = \sum_{oriented\, edges(i,j)} \cot \alpha_{ij} |u_i - u_j|^2, \tag{5}$$

$$E_\chi = \sum_{j \in N(i)} \frac{\cot \gamma_{ij} + \cot \delta_{ij}}{|x_i - x_j|^2} (u_i - u_j)^2 \tag{6}$$

in which α_{ij} is the opposite left angle of edge (i, j) on the same triangular, γ_{ij} and δ_{ij} are the angles on the both side of edge (i, j) near vertex x_j. In this way, the distortion measure E can be defined to be

$$E = \lambda E_A + \zeta E_\chi \tag{7}$$

in which λ and ζ are parameters. By minimizing E, we can get a smooth parameterization.

3.3 Surface Curvature

Curvature is an important quantity in differential geometry for assessing how a surface deviates from a plane. In the human face surface, the curvature values contain the personal features that could be used for recognition.

We define $N : S \to \mathbb{S}^2 \subseteq \mathbb{R}^3$ to be the *normal map* giving unit vector at each point p. Suppose C is a regular curve on S, p is a point on S and k is the curvature of C at p. We set $\cos \theta = \langle n, N \rangle$, where N is the normal vector to S at p and n is normal to C. $k_n = k \cos \theta$ is called the *normal curvature* of C at p. The *principal curvatures* at p are the maximum and minimum of the normal curvature, denoted as k_1 and k_2 respectively. The *mean curvature* at p is defined to be $H = \frac{1}{2}(k_1 + k_2)$.

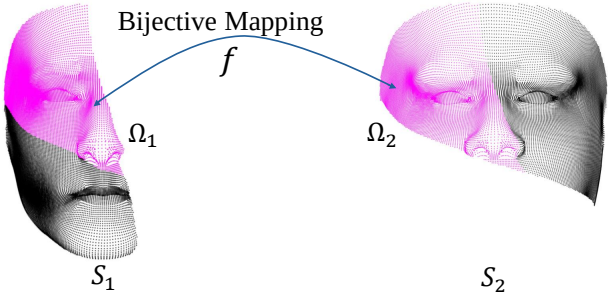

Figure 2: Demonstration of the surface matching problem. S_1 and S_2 are two partial faces with similar parts. Ω_1 and Ω_2 are the intercepted parts and labeled in magenta. The goal is to find a bijective mapping f such that the regional correspondence can be constructed for Ω_1 and Ω_2.

4 Deep Surface Registration of Partial Faces

The problem of partial surface correspondence and registration is highly significant, particularly in scenarios with limited data availability, as not all situations are ideal. To tackle this problem, we initiate our analysis by introducing the subsequent matching problem of partial surfaces.

Problem. *Given two surfaces S_1 and S_2, where S_1 and S_2 has similar regions. Suppose there exist regions Ω_1 and Ω_2 such that $\Omega_1 \subseteq S_1$ and $\Omega_2 \subseteq S_2$ respectively with similar features, the problem is to find an optimal bijective mapping $f : \Omega_1 \to \Omega_2$ such that $f(\Omega_1) = \Omega_2$.*

To visualize this problem, we demonstrate it using human faces as examples in Fig. 2. In this paper, we are introducing a deep learning based method for finding the optimal bijective mapping f for partial faces' matching problem, which is then applied to facial recognition.

4.1 Framework Overview

In this section, we present a detailed overview of our framework for partial face registration, and the strategy is shown in Fig. 3.

Our method aims to take a mean face as the template and find the optimal mapping that registers the partial face to the template. In Fig. 3, S_1 and S_2 are two partial faces that share similar regions. For each partial face, our model could generate a quasi-conformal mapping f_1, which is bijective, and map the partial face S_1 to the corresponding region on template face T. By applying the same method to the partial face S_2, we obtain a bijective quasi-conformal mapping f_2. Consequently, we can compute an inverse mapping of f_2 and compose it with f_1. This enables us to register the partial face S_1 to S_2 by mapping $f_1 \cdot f_2^{-1}$.

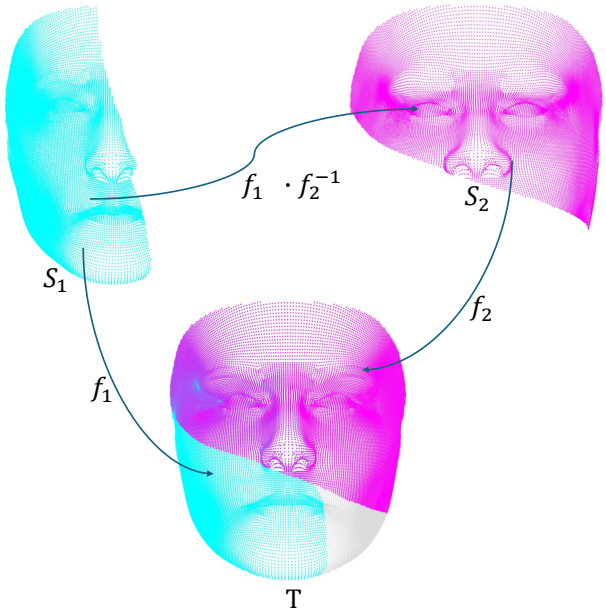

Figure 3: Demonstration of the strategy for solving partial surface correspondence problem. S_1 and S_2 are two partial faces in cyan and magenta, respectively. T is the template face in gray. f_1 and f_2 are bijective mappings.

4.2 Method Overview

In this section, we introduce the details of finding the optimal mapping f for mapping a partial face to the corresponding region on the template face T. The overview of it is shown in Fig. 4. Initially, we parameterize the partial face to the 2D domain by conformal and quasi-conformal mapping with the least angle distortion. Subsequently, a network is constructed to identify the landmarks of the parameterized face and ascertain the existence of each point. The final step involves feeding the output from the preceding network, along with the parameterized partial face, into the registration network. This process facilitates the acquisition of appropriate Beltrami Coefficients, which in turn generate a corresponding quasi-conformal mapping to register the input face to the template face, as shown in Fig. 4. Details for each component will be illustrated in the following parts.

4.2.1 Parameterization Method

The partial face is a 3D surface mesh, and to adopt the learned method, we need to parameterize it into the 2D domain. We parameterize the 3D mesh conformally and then use the quasi-conformal theory to get a visualizable face mesh while minimizing the angle distortion and keeping the majority of information of the surface mesh as shown in Fig. 5.

Initially, we adopt the Discrete Natural Conformal Parameterization(DNCP) in [11] and thus get a free boundary map from the surface. The mapping generated by DNCP is conformal, which preserves every angle of the mesh. However, as shown in Fig. 5, the parameterized face is hard to visualize as a face and also hard to determine the location of eyes or mouth; thus, we are going to use quasi-conformal theory to modify it by using an approach called least-squares quasi-conformal map (LSQC)[34, 52] with proper boundary conditions. Suppose $f : \Omega \subset \mathbb{C} \to \Omega' \subset \mathbb{C}$ is a quasi-conformal map and $f = u + iv$, $\mu_f = \rho + i\tau$ where u, v, ρ and τ are real-valued functions. We can transfer the Beltrami equation to

$$\begin{pmatrix} u_x \\ u_y \end{pmatrix} = \begin{pmatrix} 0 & 1 \\ -1 & 0 \end{pmatrix} A \begin{pmatrix} v_x \\ v_y \end{pmatrix}, \tag{8}$$

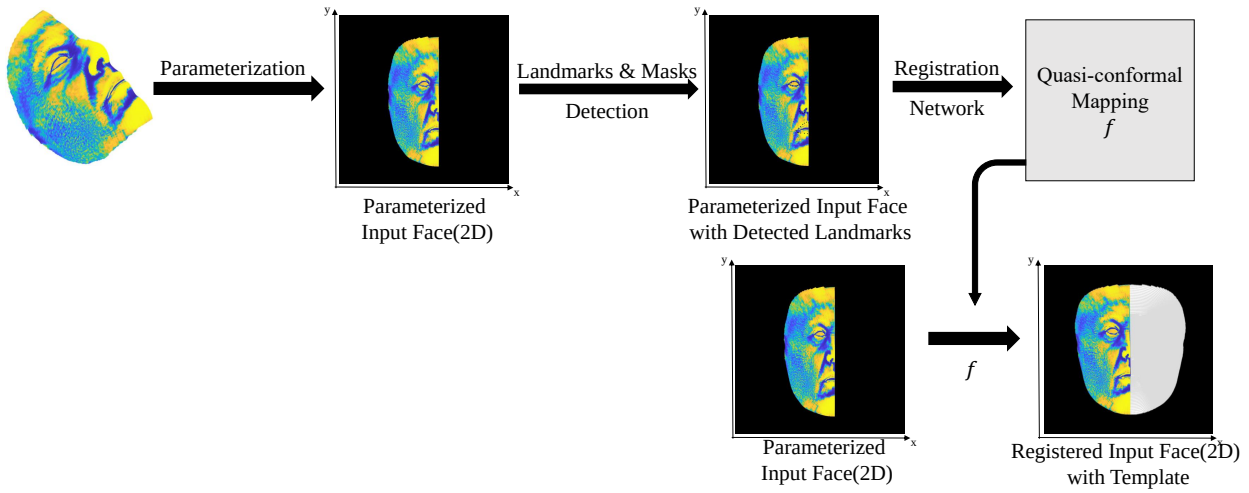

Figure 4: Demonstration of the framework for registration. The first row demonstrates how we generate a quasi-conformal mapping based on the input face mesh. Then, we demonstrate how the mapping registers an input face mesh to the template face.

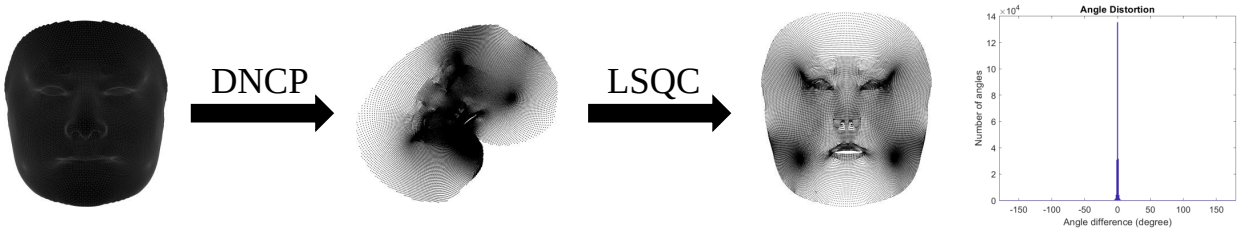

Figure 5: The flow on the left demonstrates the parameterization by discrete natural conformal parameterization(DNCP) and modified by least-squares quasi-conformal map (LSQC). The chart on the right shows the angle distortion which is small.

in which

$$A = \frac{1}{1-|\mu|^2}\begin{pmatrix}(\rho-1)^2+\tau^2 & -2\tau \\ -2\tau & (1+\rho)^2+\tau^2\end{pmatrix}. \tag{9}$$

By the relation $u_{xy} = u_{yx}$, we can get the equation

$$\nabla \cdot (A\nabla v(z)) = 0,\ \nabla \cdot (A\nabla u(z)) = 0. \tag{10}$$

These are the Euler-Lagrange equations of the following two Dirichelet-type energies respectively:

$$E_A(u) = \frac{1}{2}\int_\Omega \|A^{1/2}\nabla u\|^2,\ E_A(v) = \frac{1}{2}\int_\Omega \|A^{1/2}\nabla u\|^2. \tag{11}$$

Here we introduce the energy E_{LSQC} from [34], and we set the boundary of Ω to be mapped to a given boundary and get a quasi-conformal map from it by minimizing:

$$\begin{cases} E_{LSQC}(u,v) = \frac{1}{2}\int_\Omega \|P\nabla u + JP\nabla v\|^2 dxdy \\ f(\partial\Omega) = \partial\Omega' \end{cases}, \tag{12}$$

in which

$$P = \frac{1}{\sqrt{1-|\mu|^2}}\begin{pmatrix}1-\rho & -\tau \\ -\tau & 1+\rho\end{pmatrix} \text{ and } J = \begin{pmatrix}0 & -1 \\ 1 & 0\end{pmatrix} \tag{13}$$

It is observed that $P^T P = A$ and the Beltrami equation holds if and only if $E_{LSQC}(u, v) = 0$. There is a relationship between $E_A(u)$, $E_A(v)$, $E_{LSQC}(u, v)$ and $\mathscr{A}(u, v)$. $\mathscr{A}(u, v)$ is the area of $\Omega' = f(\Omega)$:

$$E_A(u) + E_A(v) - E_{LSQC}(u, v) = \mathscr{A}(u, v) = \int_\Omega (u_x v_y - v_x u_y) dxdy \tag{14}$$

In our setting, the face surface is discretized, and f is linear on each triangular face. Thus, we have μ constant on each face. On an oriented triangular face $T = [w_0, w_1, w_2]$, the gradient of a function $f = (f_0, f_1, f_2)$ is given by:

$$\nabla f = \frac{1}{2Area(T)} \begin{pmatrix} 0 & -1 \\ 1 & 0 \end{pmatrix} \sum_{i=0,1,2} f_i (w_{2+i} - w_{1+i}) \tag{15}$$

where the index should modulo 3. In this way, $E_A(u)$ and $E_A(v)$ can be discretized by summing over all faces which could be expressed with the generalized Laplacian matrix $\mathscr{L}_\mu$:

$$E_A(u) = u^T \mathscr{L}_\mu u,\ E_A(v) = v^T \mathscr{L}_\mu v. \tag{16}$$

We can also discretize the area matrix from Equ.14 by some skew-symmetric matrix U:

$$\mathscr{A}(u, v) = \begin{pmatrix} u^T & v^T \end{pmatrix} \begin{pmatrix} 0 & U \\ -U & 0 \end{pmatrix} \begin{pmatrix} u \\ v \end{pmatrix} \tag{17}$$

We can derive a symmetric matrix N:

$$N = \begin{pmatrix} \mathscr{L}_\mu & 0 \\ 0 & \mathscr{L}_\mu \end{pmatrix} - \begin{pmatrix} 0 & U \\ -U & 0 \end{pmatrix} \tag{18}$$

In this way, the energy E_{LSQC} can be discretized to be:

$$E_{LSQC}(u, v) = \begin{pmatrix} u^T & v^T \end{pmatrix} N \begin{pmatrix} u \\ v \end{pmatrix} \tag{19}$$

To solve the corresponding mapping, we set $\mu = 0$ with landmark constraints. The aim of this step is to have a 2D face mesh with a proper shape for visualization. Suppose the input 3D face mesh is M_0 and the boundary points are $\partial M_0 = \{m_0, m_1, ..., m_k\}$, in which $m_i = (x_i, y_i, z_i)$. We project the boundary points of the face mesh to the 2D domain as $\hat{m}_i = (x_i, y_i)$. Since we parameterize the mesh M_0 by DNCP first, we denote the parameterized face mesh to be M_1 and the boundary points are $\partial M_1 = \{n_0, n_1, ..., n_k\}$. In this way, we are solving the following problem:

$$\begin{cases} E_{LSQC}(u, v) = \begin{pmatrix} u^T & v^T \end{pmatrix} N \begin{pmatrix} u \\ v \end{pmatrix} \\ f(n_i) = \hat{m}_i, \quad n_i \in \partial M_1 \end{cases}. \tag{20}$$

Minimizing the energy E_{LSQC} could generate a mapping satisfying the input value μ if there are no boundary constraints. However, due to the added boundary conditions, very few angle distortions are introduced. In this way, the Beltrami coefficients μ would close to zero, and the mapping could be quasi-conformal, as shown in Fig. 5.

4.2.2 Landmark Detection

In this section, we outline our proposed Landmark Detection Network (LD-net) architecture, designed specifically for detecting significant points on a parameterized partial face. The detected landmarks will be used to assist the registration process.

We previously introduced the process for flattening the partial face using quasi-conformal theory. We also computed the curvature for each vertex, storing this data for future use. To leverage the capabilities of convolutional neural networks, we transformed the parameterized data into the image domain, with pixel values determined by their corresponding curvature values. The rest of the pixels are remaining zero. This transformation allows us to easily use the data as input for our landmark detection network.

Besides recording the vertex value on the image domain, we also save the location and the existence of the landmark points as labels for the supervised training. In the inference part, the input data is a partial face on the image domain,

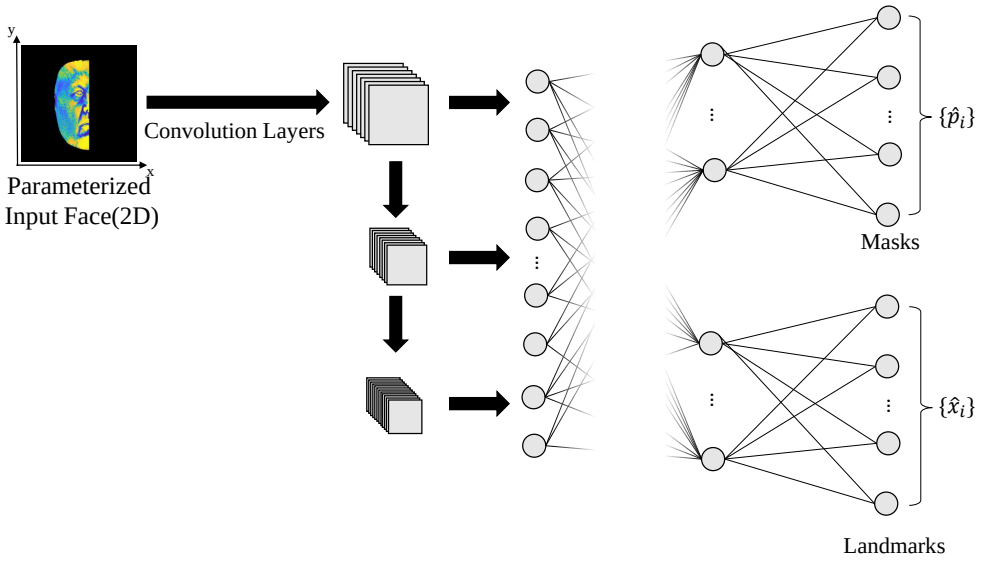

Figure 6: Demonstration for the LD-net. The input parameterized partial faces pass through convolution layers, and we take features from different scales and concatenate them into a column. Then we take the column data into two different multilayer perceptrons then generate the output masks and landmark locations.

and the objective of this network extends beyond merely determining point locations; it also involves confirming the presence of each point. The structure of our proposed network is illustrated in Fig. 6.

We first pass the smoothed image with curvature value on each vertex into convolution layers as shown in Fig. 6. Inspired by the structure by [17], we take the mean value of each channel at different stages and concatenate it to be a column for further process. The advantage is that the features at different scales are all taken into the multi-layer perceptron(MLP). Next, we take the concatenated value to two MLPs separately, and MLPs could learn from the features to generate the location and the existence of the landmarks. In the inference part, we take the detected prominent points with probability over 90% as existing.

Loss Function: For the training of LD-net, we adopt a supervised mode. The loss function of this network is as follows:

$$\mathscr{L}_{\text{LD}} = \frac{\alpha}{N}\sum_{i}^{N} -[\hat{p}_i \cdot \log(p_i) + (1-\hat{p}_i)\cdot\log(1-p_i)] + \frac{\beta}{N}\sum_{i}^{N}\|(\hat{x}_i - x_i)\odot p_i\|, \tag{21}$$

in which N is the number of prominent points predefined on the face, $\hat{p}_i$ and $\hat{x}_i$ are the output mask probability and landmark locations for the i-th point from the network, p_i and x_i are the label mask and label location for the i-th point. In our setting, the predicted $\hat{p}_i \in [0,1]$ and the labeled $p_i = 0$ or 1.

The first term in Equ. 21 is designed for the existence prediction. The network generated the probability of the existence of each point, and we adopted the cross-entropy loss between the output and the label in the training part. The second term constrains the distance between the output location and the labeled locations.

4.2.3 Registration

As introduced in the Section Mathematical Background, a quasi-conformal mapping is bijective when the Beltrami coefficient μ is less than 1, and we can easily get its inverse mapping. Based on this theory, we will introduce the procedure for registration between different partial face meshes in this part.

Initially, as shown in Fig. 7, we define the mean face as the template. Then, we design a network that is able to take the parameterized face and detected landmarks as input, and by using the Coefficients Prediction Network, we generate the Beltrami coefficients for producing the quasi-conformal mapping to register the input face to the template. To generate the quasi-conformal mapping in a fast and accurate way, we use the Beltrami Solver Network introduced by Chen et al.[8]. We demonstrate its structure in Fig. 9. In this way, different face meshes could be registered to the template mesh, and thus, we can easily compute its inverse mapping, which allows us to compare differences between face meshes.

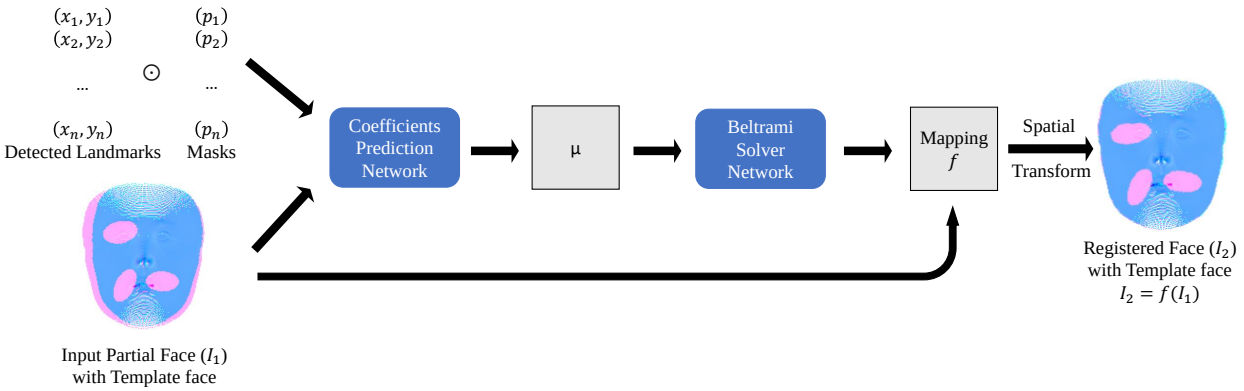

Figure 7: Demonstration for the registration process. One path takes the detected landmarks' locations and masks as input, and the second path's input is the partial face. Template face is NOT the input of the Coefficient Prediction Network(CP-net). Here is for visualization and comparison. The CP-net generates the Beltrami Coefficient μ, and the Beltrami Solver Network generates the quasi-conformal mapping f from μ. Then we can register the input partial face by f to the template face.

Next, we introduce the details of the Coefficient Prediction Network as shown in Fig. 8. We separate the input into two paths for landmarks and parameterized faces. For the Landmark Encoder, we take the detected landmarks and masks as input and use fully connected layers to process and then reshape them into 2D channels. The input partial face on the second path is in the image domain, and we pass it through the convolutional layers and concatenate it with the reshaped output from the Landmark Encoder. To preserve the bijectivity and keep the least distortion in the generated mapping, we use an activation function at the end of the Decoder to suppress the norm of Beltrami Coefficients to be less than 1 which represents no folding, and the lower, the better.

The following activation function Φ is used:

$$\Phi(m)(T) = \frac{e^{|m(T)|} - e^{-|m(T)|}}{e^{|m(T)|} + e^{-|m(T)|}} e^{iarg(m(T))},$$

in which m is the output from the last layer and $m(T)$ is a complex number on triangular face T. In this way, We have $\|\Phi(m)\|_\infty < 1$.

Loss Function: To solve the quasi-conformal mapping from the generated Beltrami Coefficent μ, we use the BS-Net from [8] which is pre-trained. In the training process, we take μ, $\nabla\mu$, landmark loss, and curvature loss into consideration, which is specified in Equ. 22. The usage of μ and $\nabla\mu$ in the first two terms of Equ. 22 is to minimize the distortion and have a smooth map for registration. The third term is the landmark loss and the aim is to register the existing prominent points to their corresponding target. The last term is the curvature loss, which ensures the partial face can be registered even with no 1-to-1 correspondence. Thus, in the computation of the last term, we only compute the intercepted parts of the registered face and the template face.

$$\mathscr{L}_{Reg} = \frac{\kappa}{N}\sum_{i=1}^{N}\|\mu_i\|_2^2 + \frac{\tau}{N}\sum_{i=1}^{N}\|\nabla\mu_i\|_2^2 + \frac{\varsigma}{M}\sum_{i=1}^{M}\|(x_i - \hat{x}_i)\odot p_i\|_2^2 + \sigma(I_2 \cdot P_{I_2\cap(I_1\cdot f^\mu)} - I_1 \cdot f^\mu)^2 \tag{22}$$

in which x_i is the target points and $\hat{x}_i$ are the registrated points. M and N are the number of prominent points and the number of triangular faces separately. p_i is the input mask for the prominent point and $p_i = 0$ or 1. If the output probability from the LD-net is larger than 90%, $p_i = 1$. Otherwise $p_i = 0$. Since the μ_i and $\nabla\mu_i$ are defined on each triangular face. I_1 represents the starting face's curvature, and I_2 represents the channel of the target face's curvature. $P_{I_2\cap(I_1\cdot f^\mu)}$ is the mask for overlapping points of the target face mesh I_2 with the registered face $I_1 \cdot f^\mu$. f^μ is the mapping generated from μ by BSnet.

5 Recognition

With our approach, we are able to determine the existence and location of features in each input partial face, facilitating their registration to the template. By aligning the registered partial faces, we can perform recognition through the overlapping of features. We demonstrate it in Fig. 10.

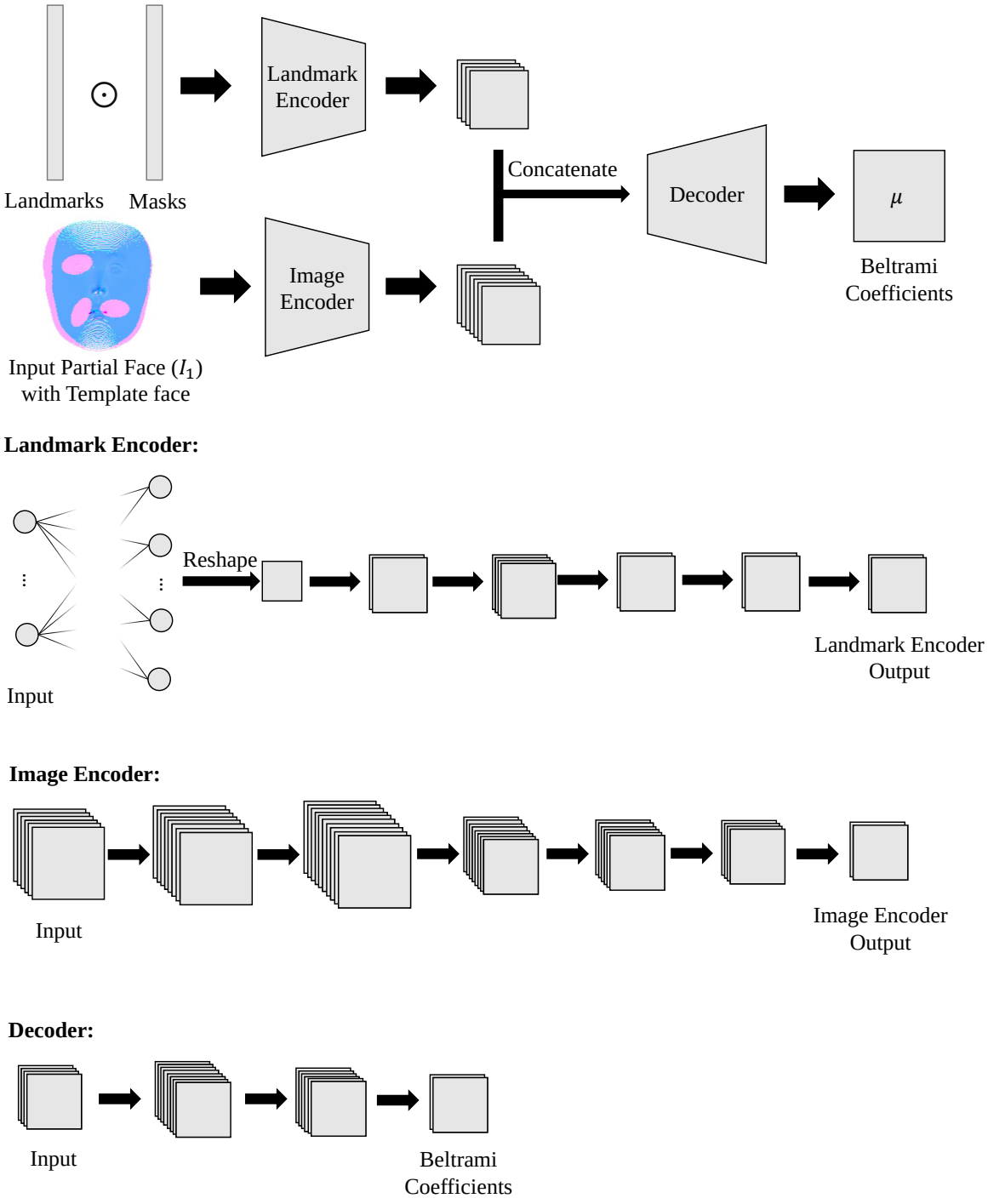

Figure 8: Demonstration for the Coefficient Prediction Network. The input is separated into two paths. The first one is taking landmarks and masks as input to the Landmark Encoder, which consists of the fully connected layers, and then reshaping the output to 2D. The second path takes the input partial face into the Image Encoder which consists of the convolutional neural networks. Then, the reshaped features are concatenated and passed through the Decoder to get the Beltrami coefficients μ. The Decoder consists of the transposed convolutions, and we use an activation function to keep each output value lower than 1 to generate a bijective quasi-conformal mapping.

To perform the 3D face recognition, we adopt the algorithm proposed by Marras et al.[30] which introduced how to recognize a face by using the azimuth angle of surface normals. In this part, we use the facial features for recognition.

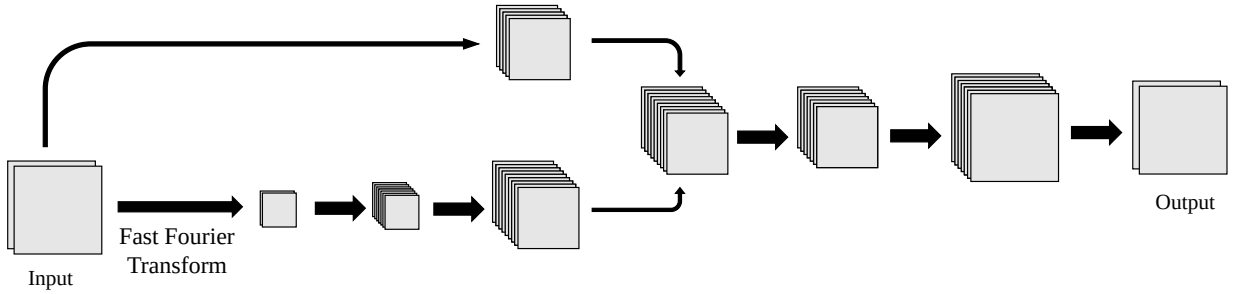

Figure 9: Demonstration of the structure of BSnet from [8].

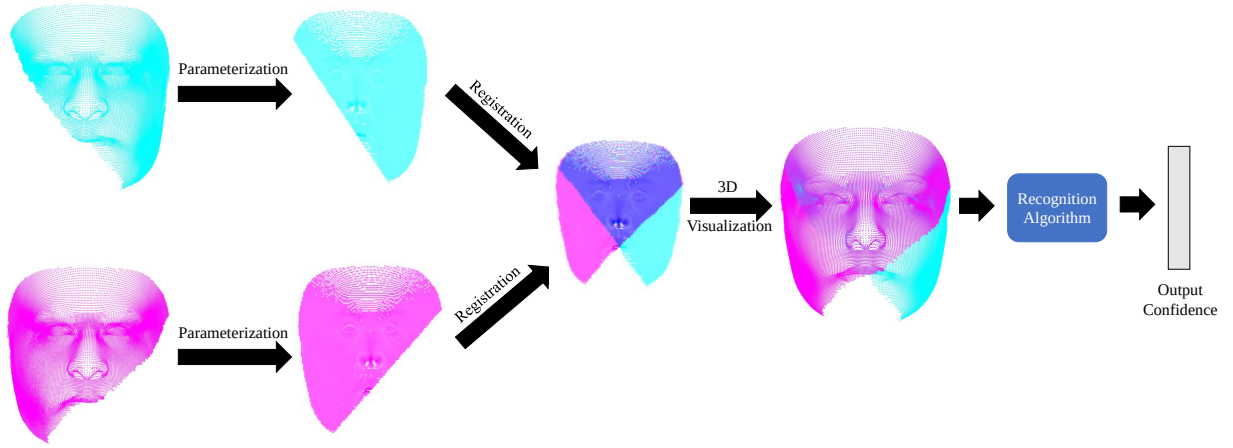

Figure 10: Demonstration for the registration process of two faces. The first column consists of two input 3D faces and the second column are their corresponding parameterized faces. The third column is the registered result after two faces pass through our model separately. The fourth column is the 3D visualization of the registered faces. We use the intercepted landmarks' normal vector to compute the distance and generate the recognition confidence.

The normal field is defined as a set of local surface normals $n(\boldsymbol{x}) = (n_x(\boldsymbol{x}), n_y(\boldsymbol{x}), n_z(\boldsymbol{x}))$ and $\|n(\boldsymbol{x})\| = 1$, where $\|\cdot\|$ is the $\mathscr{L}_2$ norm. The azimuth angle is defined as $\phi(\boldsymbol{x}) = \arctan \frac{n_y(\boldsymbol{x})}{n_x(\boldsymbol{x})}$. Then we can define the cosine-based dissimilarity measure between two vectors of azimuth angles $\boldsymbol{\phi}_i$ and $\boldsymbol{\phi}_j$ as:

$$d^2(\boldsymbol{\phi}_i, \boldsymbol{\phi}_j) \triangleq \sum_{\boldsymbol{x}} \{1 - cos[\phi_i(\boldsymbol{x}) - \phi_j(\boldsymbol{x})]\}$$

in which $\boldsymbol{x}$ are selected landmarks for recognition. Details for the experiment will be shown in the following part.

6 Experiments

6.1 Landmark Detection

Dataset. To train our model, we first generate faces by an CelebA dataset [27] and 3D Morphable Model (3DMM)[10]. To start, we generate the reconstructed faces from the image as shown in 11.

We generate 20000 face meshes and randomly cut the faces in different ways. The first dataset is generated by cutting off part of the faces, which means the output is still genus-1. The second dataset is generated by cutting off holes in random sizes and locations on the face. Then, the generated parameterized surfaces are interpolated on the image domain with its mean curvature value on each vertex.

Benchmarks. We evaluate our model on the above-mentioned generated datasets. The interpolated images are the size of 256 by 256. The mesh surface template consists of 35709 vertexes and 70865 facets. To increase the robustness of

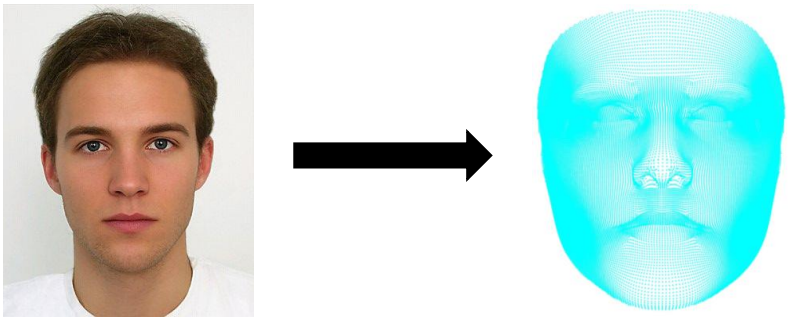

Figure 11: Demonstration for generating 3D meshes from image [10]. The image on the left is the original one and the image on the right is the mesh generated from the input image.

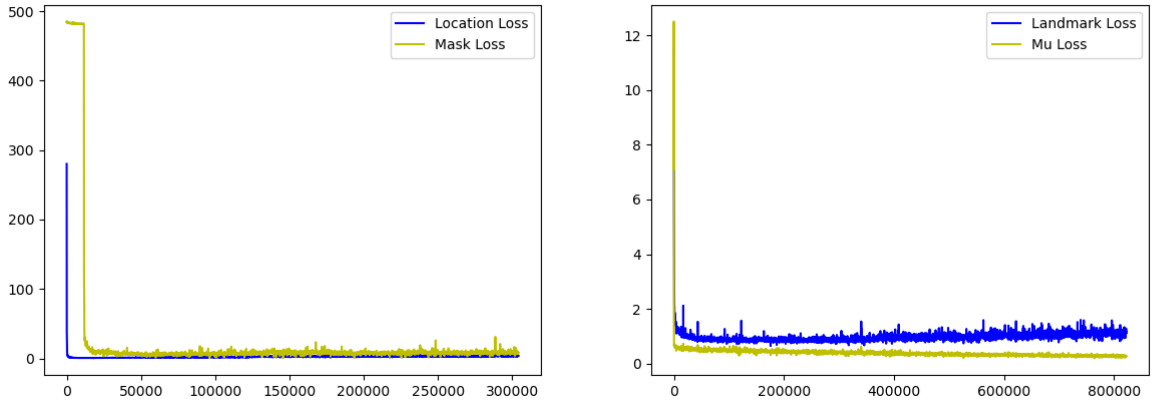

Figure 12: Demonstration for the training loss of the LD-net(Left) and Reg-net(Right). The value on the vertical axis is the error and the value on the horizontal axis is the training step.

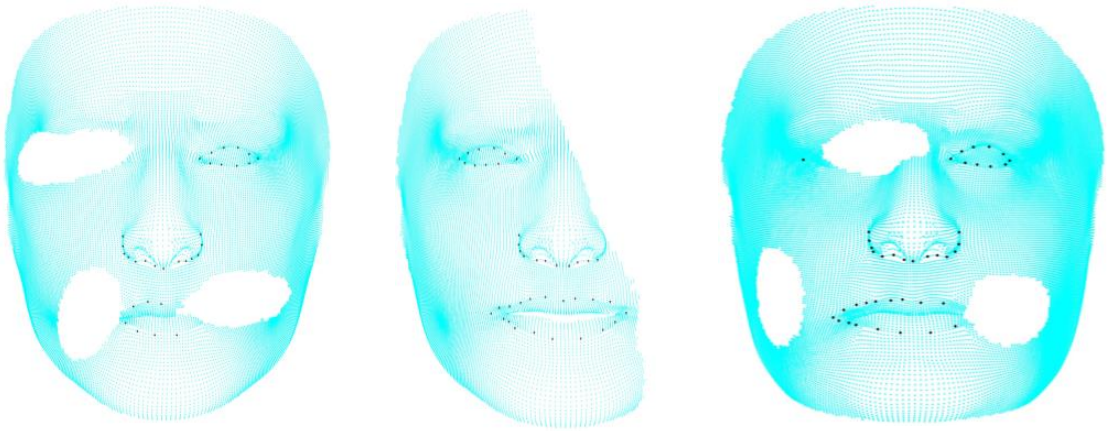

Figure 13: Demonstration for landmarks detection. The black points are the detected facial features.

our model, every parameterized face will be rotated and translated randomly. The training data and testing data are in the ratio of 5:1.

In training, we train the location-predicting path for the initial 50 epochs by using only landmark constraints. Then we add the mask loss gradually from epoch 50. Here you can see the loss in Fig. 12.

	Method	Landmark Loss	Std. of Landmark Loss	Mask Accuracy	Std. of Mask
Partial	LD-net	0.935	0.057	98.2%	0.46%
	SBR [13]	87.537	0.025	\	\
	AWing [44]	13.354	0.151	\	\
	PFLD [17]	1.167	0.051	\	\
	SRT [12]	1.088	0.042	\	\
Holes	LD-net	1.066	0.042	99.0%	0.41%
	SBR [13]	87.529	0.015	\	\
	AWing [44]	14.066	0.097	\	\
	PFLD [17]	1.868	0.027	\	\
	SRT [12]	0.947	0.037	\	\

Table 1: Comparison with the existing method for facial landmark detection on the dataset of partial faces and the dataset of faces with holes. We also list the standard deviation while testing. The best result is shown in red, second best in blue.

In table 1, we compare our method with other facial landmark detection networks. All the networks are trained on partial faces and face with holes, and all the compared networks have no mask output. The testing set consists of 5000 images, and the images are not contained in the training set.

As shown in table 1, our model outperforms all other methods. SRT and PFLD can also achieve comparable loss in landmark loss but have no mask output for the prominent points' detection. SBR and AWing failed in this sort of dataset.

6.2 Registration

For the registration process, we use the same dataset as we used for detection. In the training of the registration network, we set a face with no missing part as a template and register all the input faces to the template by a generated quasi-conformal mapping. Since the quasi-conformal mapping is bijective and we can easily get the inverse mapping based on the output quasi-conformal mapping.

In Fig. 12, we demonstrate the training loss of the registration network. We set the constraint of value μ at a low level while starting training and adding up its parameter gradually. It is easy to see that value of μ will drop close to zero at the compensation of a little bit higher rigid error.

In Fig. 14, we demonstrate our model is able to register a partial face to the template full face and have all landmarks aligned.

Since every partial face can be registered to the template and the generated mapping is quasi-conformal, we can get its inverse mapping easily. Thus, for every input partial face, after being registered by our model, we can easily analyze the overlapping features for recognition. In Fig. 10, we demonstrate two different partial faces which are registered together.

In Fig. 15, we demonstrate that if two faces with very few overlapping, we can also register both faces and easy to analyze the overlapping features for recognition. We will test our model for recognition in the next part.

6.3 Recognition

Dataset. We utilize the Labeled Faces in the Wild (LFW) dataset, which comprises 13,233 facial images from 5749 identities. The dataset includes a diverse collection of real-world facial images captured under various conditions, and we select the ones that are easier for 3DMM to reconstruct the 3D face meshes. This enables comprehensive evaluations of our approach. This labeled large dataset allows us to assess the performance and robustness of our method effectively.

The data we use for recognition is Labeled Faces in the Wild(LFW)[21] and we mainly compare with the non-rigid ICP[1] and the result is shown in 2. To be precise, our method is trained on the previous dataset(use the dataset name) so the LFW dataset is unseen for our model. In Table 2, we can achieve the recognition accuracy of 91.73%. It is acceptable that it is not close to 100% since the overlap landmarks could reduce to just a few points. Besides testing the recognition accuracy, we also perform statistical analyses of the result. Suppose x_0 is a vector that contains the distances of the same person and x_1 contains the distances between different persons. Our hypothesis is that H_0: the mean of x_0 equals the mean of x_1, H_1: the mean of x_0 less than the mean of x_1. In Table 2, the p-value of our output is 3.59×10^{-13} and it can be fully convinced that our method could recognize different people reliably.

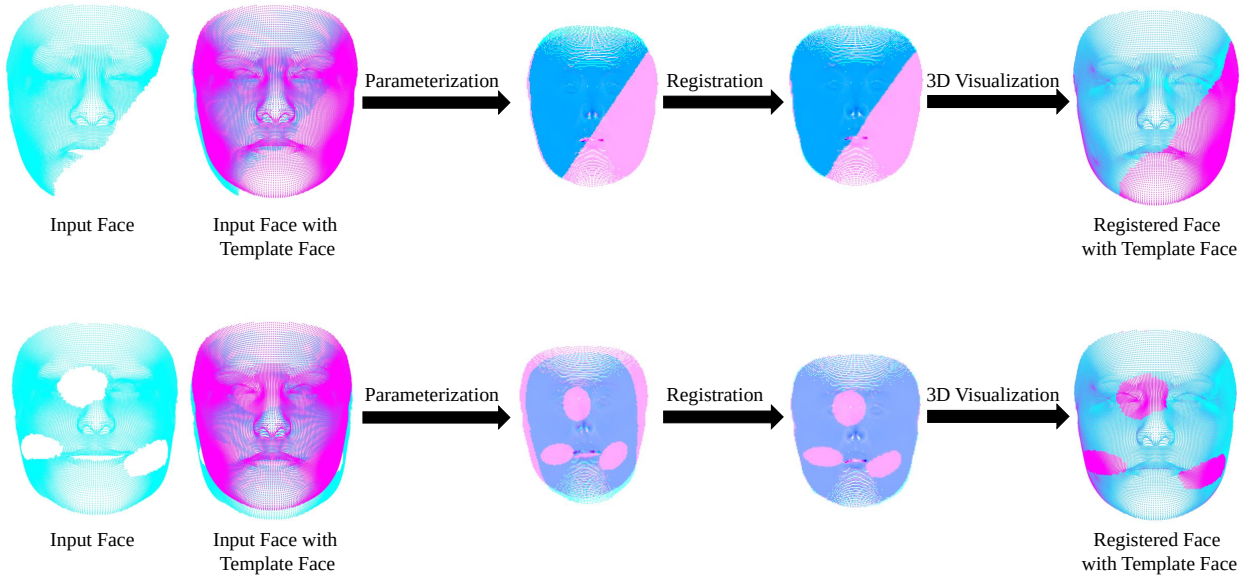

Figure 14: On the first column, the input partial face is in pink and the template face is in cyan. The overlapping part is in pink. The second column is the registered partial face with the template face. It can be viewed that the facial features can be aligned with the template. The third column is the mapping generated by our model.

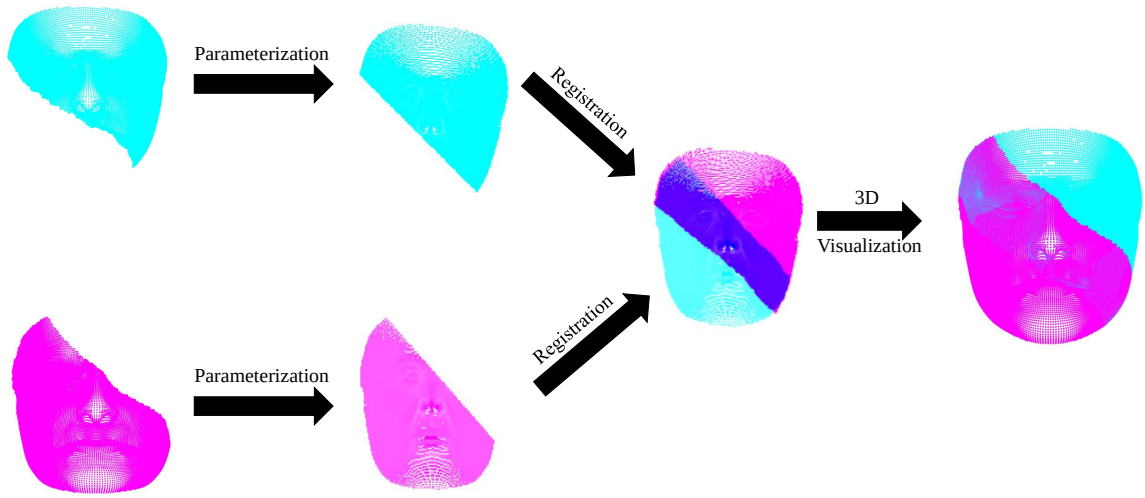

Figure 15: Demonstration of two faces with few overlapping.

7 Conclusion

In conclusion, this work emphasizes the importance of 3D facial analysis and introduced effective techniques for analyzing and comparing partial faces. By using quasi-conformal theory, we achieved accurate parameterization of 3D partial face meshes with minimal distortion. Our study introduced an automated method for detecting landmarks and prominent points on partial faces, eliminating the need for manual annotation. This allowed for precise alignment of partial faces, enabling comprehensive analysis. By generating Beltrami coefficients and applying quasi-conformal mapping, we ensured accurate comparisons between partial faces while preserving bijectivity. The derived distribution

Method	Recognition Accuracy	T-test	Time
Our Method	91.73%	3.59×10^{-13}	0.102
Non-rigid ICP(ϵ=1)	51.24%	0.8244	116.719
Non-rigid ICP(ϵ=0.1)	51.65%	0.0997	315.766
Non-rigid ICP(ϵ=0.01)	52.07%	0.6888	1.56×10^{3}

Table 2: Comparison with non-rigid ICP with different parameters for recognition. Our network's performance is far better than non-rigid ICP with any parameter. The t-test shows that the distance of the same person is significantly lower than the distance of the different person after being processed by our model.

of optimal Beltrami coefficients can be used for metric learning in partial face registration problems. Extensive experiments have demonstrated the effectiveness of our approach to landmark detection and partial face registration. Overall, this research contributes to advancing 3D facial analysis by providing efficient techniques for parameterization, landmark detection, and registration of partial faces. These findings have potential implications in various fields, such as biometrics, computer vision, and human-computer interaction. Further research can build upon these methods to improve the accuracy and efficiency of facial analysis.

Acknowledgement

This work is partially supported by HKRGC GRF (Project ID: 14306721).

References

[1] Brian Amberg, Sami Romdhani, and Thomas Vetter. Optimal step nonrigid icp algorithms for surface registration. In *2007 IEEE conference on computer vision and pattern recognition*, pages 1–8. IEEE, 2007.

[2] Kari Astala, Tadeusz Iwaniec, and Gaven Martin. Elliptic partial differential equations and quasiconformal mappings in the plane (pms-48). In *Elliptic Partial Differential Equations and Quasiconformal Mappings in the Plane (PMS-48)*. Princeton University Press, 2008.

[3] Amit Bracha, Thomas Dagès, and Ron Kimmel. On partial shape correspondence and functional maps. *arXiv preprint arXiv:2310.14692*, 2023.

[4] Alan Brunton, Augusto Salazar, Timo Bolkart, and Stefanie Wuhrer. Review of statistical shape spaces for 3d data with comparative analysis for human faces. *Computer Vision and Image Understanding*, 128:1–17, 2014.

[5] Xavier P Burgos-Artizzu, Pietro Perona, and Piotr Dollár. Robust face landmark estimation under occlusion. In *Proceedings of the IEEE international conference on computer vision*, pages 1513–1520, 2013.

[6] Dongliang Cao, Paul Roetzer, and Florian Bernard. Unsupervised learning of robust spectral shape matching. *arXiv preprint arXiv:2304.14419*, 2023.

[7] Hei-Long Chan, Hoi-Man Yuen, Chun-Ting Au, Kate Ching-Ching Chan, Albert Martin Li, and Lok-Ming Lui. Quasi-conformal geometry based local deformation analysis of lateral cephalogram for childhood osa classification. *arXiv preprint arXiv:2006.11408*, 2020.

[8] Qiguang Chen, Zhiwen Li, and Lok Ming Lui. A deep learning framework for diffeomorphic mapping problems via quasi-conformal geometry applied to imaging. *arXiv preprint arXiv:2110.10580*, 2021.

[9] Fernando De la Torre and Jeffrey F Cohn. Facial expression analysis. *Visual analysis of humans: Looking at people*, pages 377–409, 2011.

[10] Yu Deng, Jiaolong Yang, Sicheng Xu, Dong Chen, Yunde Jia, and Xin Tong. Accurate 3d face reconstruction with weakly-supervised learning: From single image to image set. In *Proceedings of the IEEE/CVF conference on computer vision and pattern recognition workshops*, pages 0–0, 2019.

[11] Mathieu Desbrun, Mark Meyer, and Pierre Alliez. Intrinsic parameterizations of surface meshes. *Comput. Graph. Forum*, 21(3):209–218, 2002.

[12] Xuanyi Dong, Yi Yang, Shih-En Wei, Xinshuo Weng, Yaser Sheikh, and Shoou-I Yu. Supervision by registration and triangulation for landmark detection. 2020. doi:10.1109/TPAMI.2020.2983935.

[13] Xuanyi Dong, Shoou-I Yu, Xinshuo Weng, Shih-En Wei, Yi Yang, and Yaser Sheikh. Supervision-by-Registration: An unsupervised approach to improve the precision of facial landmark detectors. In *Proceedings of the IEEE Conference on Computer Vision and Pattern Recognition (CVPR)*, pages 360–368, 2018.

[14] Zhen-Hua Feng, Josef Kittler, Muhammad Awais, Patrik Huber, and Xiao-Jun Wu. Wing loss for robust facial landmark localisation with convolutional neural networks. In *Proceedings of the IEEE conference on computer vision and pattern recognition*, pages 2235–2245, 2018.

[15] Michael S Floater and Kai Hormann. Surface parameterization: a tutorial and survey. *Advances in Multiresolution for Geometric Modelling*, pages 157–186, 2005.

[16] Frederick P Gardiner and Nikola Lakic. *Quasiconformal teichmuller theory*. Number 76. American Mathematical Soc., 2000.

[17] Xiaojie Guo, Siyuan Li, Jinke Yu, Jiawan Zhang, Jiayi Ma, Lin Ma, Wei Liu, and Haibin Ling. Pfld: A practical facial landmark detector. *arXiv preprint arXiv:1902.10859*, 2019.

[18] Yuchen Guo, Qiguang Chen, Gary Choi, and Lok Ming Lui. Automatic landmark detection and registration of brain cortical surfaces via quasi-conformal geometry and convolutional neural networks. *arXiv preprint arXiv:2208.07010*, 2022.

[19] Juha Heinonen and Pekka Koskela. Quasiconformal maps in metric spaces with controlled geometry. *Acta Mathematica*, 181(1):1–61, 1998.

[20] Xiaobin Hu, Wenqi Ren, John LaMaster, Xiaochun Cao, Xiaoming Li, Zechao Li, Bjoern Menze, and Wei Liu. Face super-resolution guided by 3d facial priors. In *Computer Vision–ECCV 2020: 16th European Conference, Glasgow, UK, August 23–28, 2020, Proceedings, Part IV 16*, pages 763–780. Springer, 2020.

[21] Gary B. Huang, Manu Ramesh, Tamara Berg, and Erik Learned-Miller. Labeled faces in the wild: A database for studying face recognition in unconstrained environments. Technical Report 07-49, University of Massachusetts, Amherst, October 2007.

[22] Kostiantyn Khabarlak and Larysa Koriashkina. Fast facial landmark detection and applications: A survey. *Journal of Computer Science and Technology*, 22(1):e02–e02, 2022.

[23] Marek Kowalski, Jacek Naruniec, and Tomasz Trzcinski. Deep alignment network: A convolutional neural network for robust face alignment. In *Proceedings of the IEEE conference on computer vision and pattern recognition workshops*, pages 88–97, 2017.

[24] Alexandros Lattas, Stylianos Moschoglou, Baris Gecer, Stylianos Ploumpis, Vasileios Triantafyllou, Abhijeet Ghosh, and Stefanos Zafeiriou. Avatarme: Realistically renderable 3d facial reconstruction" in-the-wild". In *Proceedings of the IEEE/CVF conference on computer vision and pattern recognition*, pages 760–769, 2020.

[25] Olli Lehto and Kaarlo Ilmari Virtanen. *Quasiconformal mappings in the plane*, volume 126. Citeseer, 1973.

[26] Bruno Lévy, Sylvain Petitjean, Nicolas Ray, and Jérome Maillot. Least squares conformal maps for automatic texture atlas generation. *ACM Trans. Graph.*, 21(3):362–371, 2002.

[27] Ziwei Liu, Ping Luo, Xiaogang Wang, and Xiaoou Tang. Deep learning face attributes in the wild. In *Proceedings of International Conference on Computer Vision (ICCV)*, 2015.

[28] Changwei Luo, Zengfu Wang, Shaobiao Wang, Juyong Zhang, and Jun Yu. Locating facial landmarks using probabilistic random forest. *IEEE Signal Processing Letters*, 22(12):2324–2328, 2015.

[29] Riccardo Marin, Arianna Rampini, Umberto Castellani, Emanuele Rodolà, Maks Ovsjanikov, and Simone Melzi. Spectral shape recovery and analysis via data-driven connections. *International journal of computer vision*, 129:2745–2760, 2021.

[30] Ioannis Marras, Stefanos Zafeiriou, and Georgios Tzimiropoulos. Robust learning from normals for 3d face recognition. In *Computer Vision–ECCV 2012. Workshops and Demonstrations: Florence, Italy, October 7-13, 2012, Proceedings, Part II 12*, pages 230–239. Springer, 2012.

[31] Qiang Meng, Shichao Zhao, Zhida Huang, and Feng Zhou. Magface: A universal representation for face recognition and quality assessment. In *Proceedings of the IEEE/CVF conference on computer vision and pattern recognition*, pages 14225–14234, 2021.

[32] José Augusto Cadena Moreano and NBLS Palomino. Global facial recognition using gabor wavelet, support vector machines and 3d face models. *Journal of Advances in Information Technology*, 11(3), 2020.

[33] Patrick Mullen, Yiying Tong, Pierre Alliez, and Mathieu Desbrun. Spectral conformal parameterization. *Comput. Graph. Forum*, 27(5):1487–1494, 2008.

[34] Di Qiu, Ka-Chun Lam, and Lok-Ming Lui. Computing quasi-conformal folds. *SIAM Journal on Imaging Sciences*, 12(3):1392–1424, 2019.

[35] Di Qiu and Lok Ming Lui. Inconsistent surface registration via optimization of mapping distortions. *Journal of Scientific Computing*, 83:1–31, 2020.

[36] Evangelos Sariyanidi, Hatice Gunes, and Andrea Cavallaro. Automatic analysis of facial affect: A survey of registration, representation, and recognition. *IEEE transactions on pattern analysis and machine intelligence*, 37(6):1113–1133, 2014.

[37] Florian Schroff, Dmitry Kalenichenko, and James Philbin. Facenet: A unified embedding for face recognition and clustering. In *Proceedings of the IEEE conference on computer vision and pattern recognition*, pages 815–823, 2015.

[38] Alla Sheffer, Emil Praun, and Kenneth Rose. Mesh parameterization methods and their applications. *Found. Trends Comput. Graph. Vis.*, 2(2):105–171, 2007.

[39] Yi Sun, Ding Liang, Xiaogang Wang, and Xiaoou Tang. Deepid3: Face recognition with very deep neural networks. *arXiv preprint arXiv:1502.00873*, 2015.

[40] Yi Sun, Xiaogang Wang, and Xiaoou Tang. Deeply learned face representations are sparse, selective, and robust. In *Proceedings of the IEEE conference on computer vision and pattern recognition*, pages 2892–2900, 2015.

[41] Murat Taskiran, Nihan Kahraman, and Cigdem Eroglu Erdem. Face recognition: Past, present and future (a review). *Digital Signal Processing*, 106:102809, 2020.

[42] Luan Tran and Xiaoming Liu. Nonlinear 3d face morphable model. In *Proceedings of the IEEE conference on computer vision and pattern recognition*, pages 7346–7355, 2018.

[43] Michal Uřičář, Vojtěch Franc, and Václav Hlaváč. Detector of facial landmarks learned by the structured output svm. *VIsAPP*, 12:547–556, 2012.

[44] Xinyao Wang, Liefeng Bo, and Li Fuxin. Adaptive wing loss for robust face alignment via heatmap regression. In *Proceedings of the IEEE/CVF international conference on computer vision*, pages 6971–6981, 2019.

[45] Yue Wu and Qiang Ji. Facial landmark detection: A literature survey. *International Journal of Computer Vision*, 127(2):115–143, 2019.

[46] Tarun Yenamandra, Ayush Tewari, Florian Bernard, Hans-Peter Seidel, Mohamed Elgharib, Daniel Cremers, and Christian Theobalt. i3dmm: Deep implicit 3d morphable model of human heads. In *Proceedings of the IEEE/CVF Conference on Computer Vision and Pattern Recognition*, pages 12803–12813, 2021.

[47] Mei-Heng Yueh, Wen-Wei Lin, Chin-Tien Wu, and Shing-Tung Yau. An efficient energy minimization for conformal parameterizations. *J. Sci. Comput.*, 73(1):203–227, 2017.

[48] Wei Zeng, Lok Ming Lui, and Xianfeng Gu. Surface registration by optimization in constrained diffeomorphism space. In *Proceedings of the IEEE Conference on Computer Vision and Pattern Recognition*, pages 4169–4176, 2014.

[49] Zhanpeng Zhang, Ping Luo, Chen Change Loy, and Xiaoou Tang. Facial landmark detection by deep multi-task learning. In *Computer Vision–ECCV 2014: 13th European Conference, Zurich, Switzerland, September 6-12, 2014, Proceedings, Part VI 13*, pages 94–108. Springer, 2014.

[50] Zhanpeng Zhang, Ping Luo, Chen Change Loy, and Xiaoou Tang. Learning deep representation for face alignment with auxiliary attributes. *IEEE transactions on pattern analysis and machine intelligence*, 38(5):918–930, 2015.

[51] Yang Zhao, Yifan Liu, Chunhua Shen, Yongsheng Gao, and Shengwu Xiong. Mobilefan: Transferring deep hidden representation for face alignment. *Pattern Recognition*, 100:107114, 2020.

[52] Zhipeng Zhu, Gary PT Choi, and Lok Ming Lui. Parallelizable global quasi-conformal parameterization of multiply connected surfaces via partial welding. *SIAM Journal on Imaging Sciences*, 15(4):1765–1807, 2022.

[53] Xu Zou, Sheng Zhong, Luxin Yan, Xiangyun Zhao, Jiahuan Zhou, and Ying Wu. Learning robust facial landmark detection via hierarchical structured ensemble. In *Proceedings of the IEEE/CVF International Conference on Computer Vision*, pages 141–150, 2019.